# Depolarisation Model for a BAN Indoor Scenario

Manuel M. Ferreira, Filipe D. Cardoso
Instituto Politécnico de Setúbal, ESTSetúbal and INESC-ID
Setúbal, Portugal
manuel.ferreira@estsetubal.ips.pt
filipe.cardoso@estsetubal.ips.pt

Sławomir J. Ambroziak
Faculty of Electronics, Telecomm and Informatics
Gdańsk University of Technology
Digital Technologies Center, Gdańsk, Poland
slawomir.ambroziak@pg.edu.pl

Mariella Särestöniemi
Centre for Wireless Communications
Health Sciences and Technology, University of Oulu
Oulu, Finland
mariella.sarestoniemi@oulu.fi

Kenan Turbic
ICE, RWTH Aachen University
Aachen, Germany
turbic@ice.rwth-aachen.de

Luís M. Correia
IST/INESC-ID, University of Lisbon
Lisbon, Portugal
luis.m.correia@tecnico.ulisboa.pt

*Abstract* — **In this paper, an analysis of depolarisation in Body Area Networks for Body-to-Infrastructure communications based on a measurement campaign in the 5.8 GHz band in an indoor environment is performed. Measurements were made with an off-body antenna transmitting linearly polarised signals and dual-polarised receiving antennas carried by the user on the body. A Normal Distribution with a mean of 2.0 dB and a standard deviation of 4.3 dB is found to be the best fit for modelling cross-polarisation discrimination. The average correlation between the signals received by the orthogonally polarised antennas is below 0.5, showing that polarisation diversity can be used. A model is proposed for the average value of the standard deviation of the cross-polarisation discrimination ratio as a function of the transmitted polarisation, the mobility of users and link dynamics.**

*Keywords— Body Area Networks, Depolarisation, Indoors, Off-Body, User Mobility.*

## I. Introduction

Mobile and wireless communications are constantly evolving, being very close to the goal of connectivity everywhere and at all times. As microelectronics enables the development of semiconductors with higher levels of integration and lower energy consumption, it becomes possible to build devices with good computing resources, high autonomy, and very small dimensions. The integration of radios in these small devices enables ubiquitous networks in which all devices are interconnected. Body Area Networks (BANs) correspond to a set of wireless devices attached to the human body, being one of the latest achievements in ubiquitous and anytime communication [1]. BANs already play an important role in some applications, such as monitoring of the body's vital functions, operational scenarios in medicine, sports, military, police and civil defence, and entertainment.

The propagation of signals between an on-body antenna and an off-body antenna in a Body-to-Infrastructure (B2I) or a Body-to-Body (B2B) configuration involves many random variables. Therefore, the characterisation of the propagation channel in B2I and B2B scenarios, especially in terms of average system loss and fading, is very important for system development and design due to the influence of antennas position of the antennas on the body together with the mobility of the users and the dynamics of the environment.

There are several studies in the literature on the influence of antenna polarisation in BANs. In [2] and [3], the authors investigate how the radiation pattern and antenna polarisation affect the "path gain" between two on-body antennas. In [4], three user mobility patterns with different dynamic characteristics (walking, weak walking and running) were considered; results were obtained for nine different polarisation schemes in terms of transmitter (Tx) and receiver (Rx) orientation, for six receiver locations. In [5], a study on the propagation characteristics of creeping waves along the skin surface is presented and the performance in terms of antenna efficiency, reflection coefficient and maximum gain is compared among perpendicular, parallel and mixed polarisations relative to the skin. These studies show that polarisation perpendicular to the skin is the best for on-body communication.

In [6], by placing a Tx antenna on the body with linear polarisation and two Rx antennas outside the body (with vertical and circular polarisations), the authors investigated how different positions of the user's body affect depolarisation. It was found that the signal received by the antenna with vertical polarisation varies with body position, while the antenna with circular polarisation is virtually unaffected. The mismatch of the polarisation is, thus, influenced by the body position and the user movement.

This paper presents a study on the impact of user mobility on the propagation channel in indoor BAN scenarios. The results

of an Ultra-Wideband (UWB) measurement campaign in a B2I scenario with standing, and walking users are presented. The novelty of this work lies on the extension of the work in [7], by considering transmission with horizontally and vertically polarised signals and extending the analysis to the effects of user mobility, link dynamics and antenna visibility on depolarisation.

This paper is structured as follows. The measurement campaign, scenarios, equipment, and antennas are described in Section II. A general description of the signal propagation aspects in BANs is given in Section III, together with a discussion of antenna visibility classification, link dynamics and user mobility. The processing of the measured data is described in Section IV. Section V analyses the dependence of the cross-polarisation discrimination and its standard deviation on user mobility, link dynamics, antenna visibility and Tx polarisation. A model for depolarisation is presented in Section VI. Conclusions are drawn in Section VII.

## II. Measurement Scenario, Simulations and Setup

The environment and measurement scenarios are described in detail in [7], [8] and [9], so only a brief description is given in this section. The UWB measurements (500 MHz bandwidth) [10] were performed in the 5.8 GHz band in an empty conference room at the Gdańsk University of Technology, as shown in Fig. 1. The user moved along three parallel routes 1 m apart, with the central route, Route C, located directly in front of the Access Point (AP).

Two different user mobility conditions were considered: Standing, where measurements were taken at evenly spaced intervals of 0.5 m along each route, and Walking, where the user moved along the routes at a constant speed of about 1.3 m/s, the usual walking speed. For the Standing scenarios, 50 consecutive Channel Impulse Responses (CIR) were recorded at each position, while for Walking, measurements were repeated 10 times for each route. Two directions of movement were considered for the user: Approach, where the user moved towards the AP, and Departure, where the user moved away from the AP.
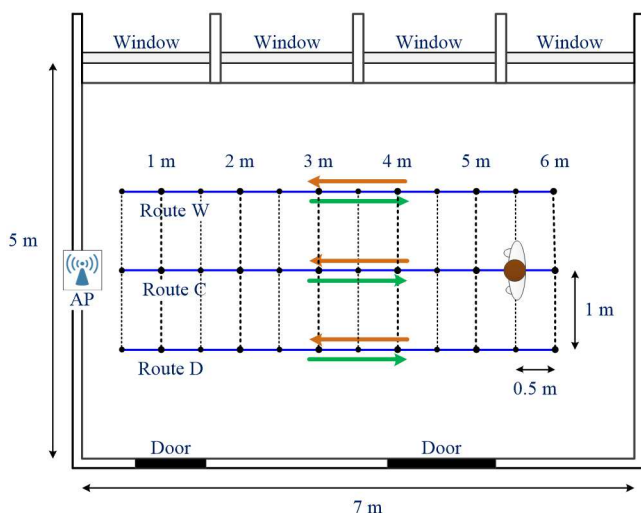


Fig. 1. Floor plan of the room with Walking routes (blue lines).

Measurements were repeated for each antenna position on the body: Chest (front of the torso, To_F), Head (left side of

head, He_L), Wrist (left lower arm, AL_L) and Leg (left lower leg, LL_L). The height of the antennas was 1.3 m, 1.7 m, 0.94 m, and 0.32 m for To_F, He_L, AL_L and LL_L, respectively.

The properties of the antennas were calculated using Dassault Simulia CST Studio Suite [11], an electromagnetic simulation software based on the Finite Integration Technique. The properties of the on-body antenna were determined using a homogeneous human voxel model with an antenna-to-body distance of 16 mm as in measurements. The properties of the AP antenna were determined by modelling a concrete wall and placing the antenna at a distance of 16 mm from the wall.

## III. Classification Parameters

### A. Scenario implications

In BANs, the dynamics of the channels depend on the scenario. For example: in a concert, users move in an environment with many people but with a very limited radius of action; in a bus, users stand in an environment with many people but with limited mobility; in a park, users walk in a relatively open area; and in fitness activities, users walk and run in an outdoor or indoor environment. In this work, channel dynamics are characterised by three different parameters: antenna visibility, link dynamics and user mobility.

Regarding the visibility of the antennas, their placement has a significant impact on the signal behaviour, as different configurations can lead to a variety of cases in terms of visibility between Tx and Rx antennas. The dynamics of the link between Tx and Rx antennas is related to the degree of movement of the different parts of the body. The mobility of the user describes how the user moves in the scenario, e.g., standing, walking, or running. The direction of the user's movement is also important, e.g., in To_F and Approach the antenna is pointed at the AP, while in Departure the user looks away from the AP and body shadowing occurs. The propagation characteristics are not the same on the left and right side of the routes, i.e., on one side there is a wall mostly covered with PVC-framed windows while on the other side there is a concrete wall, resulting in different reflections.

### B. Antenna visibility, user mobility and link dynamics

The classification of visibility between Tx and Rx antennas used in this paper follows the approach in [12], which depends on the relative position of these antennas and is divided into six categories: Line-of-Sight (LoS), Quasi-LoS (QLoS), Obstructed-LoS (OLoS) and Non-LoS (NLoS), with the two categories between LoS and NLoS further distinguishing between strong "s" and weak "w" signal strengths.

When there is no body shadowing (routes C and W on Approach and routes C and D on Departure), a strong QLoS (sQLoS) condition is verified, while in the other cases body shadowing occurs (route D on Approach and route W on Departure), corresponding to a strong OLoS (sOLoS). For ToF, antenna there are LoS and sOLoS conditions for the approach and departure scenarios.

The classification of antenna visibility for these scenarios, as a function of user movement direction, route, and antenna placement on the body, is shown in Table I.

The effect of antenna visibility was simulated by first calculating the average antenna gain in each of the visibility

zones (inHPBW, outHPBW, and shHem); an additional value of 10 dB was added for situations with body shadow [13]. Then these values were normalised assuming that the additional attenuation for LoS is 0 dB. The full set for the different visibility conditions is given in Table II; the cases found in the actual measurements are marked in bold.

TABLE I. VISIBILITY CLASSIFICATION.

| Movement | Route | On-body antenna | | | |
|---|---|---|---|---|---|
| | | To_F | He_L | LL_L | AL_L |
| Approach | C/W | LoS | sQLoS | | |
| | D | | sOLoS | | |
| Departure | C/D | sOLoS | sQLoS | | |
| | W | | sOLoS | | |

TABLE II. VISIBILITY CLASSIFICATION AND NORMALISED ATTENUATION.

| Visibility | LoS | sQLoS | wQLoS | sOLoS | wOLoS | NLoS |
|---|---|---|---|---|---|---|
| Normalised attenuation, $L_{add}$ [dB] | **0** | **6.5** | 13.0 | **31.8** | 38.3 | 63.6 |

As mentioned earlier, the user has two different mobility patterns: Standing and Walking. Regarding link dynamics, the classification follows the proposal in [12], i.e., the link dynamics is classified as Low if the antennas are located on the body on the torso or on the head, and as Medium if they are placed on the leg or on the arm. The values for classifying limb movements are based on an average human limb speed of 2 m/s [14], therefore Low, Medium and High dynamic links have values of 0, 2 and 4 m/s respectively. The classification of link dynamics according to this criterion is shown in Table III.

TABLE III. LINK DYNAMICS CLASSIFICATION.

| On-body antenna | Link dynamics |
|---|---|
| To_F | Low |
| He_L | |
| LL_L | Medium |
| AL_L | |

## IV. DATA PROCESSING

### A. CIR processing

The multipath components (MPCs) were calculated by deconvolving the CIRs with a modification of the procedure from [15] as described in [7], estimating both polarisations simultaneously for consistency. Since propagation paths depend only on antennas positions, the received MPCs for the orthogonal polarisations have the same delays but different amplitudes [16]. The ITU-R definitions of polarisation were adopted [17], i.e., co-polarisation (CP) as the polarisation component identical to the expected one, and cross-polarisation (XP) as the component orthogonal to the expected one.

For each measuring point at a certain distance from the AP, a series of measurements were taken at different times. Thus, measurements depend on the time at which they were taken, on the distance to AP and on the route. In addition to the three parallel routes (routes C, W and D), the polarisation transmitted

by the AP (V-Pol or H-Pol), the mobility of the user (Standing or Walking), the type of movement of the user (Approach or Departure) and the placement of the antenna (To_F, He_L, AL_L, LL_L) must also be taken into account. A total of 96 cases were measured, each representing a different situation.

The Rx power of each measurement, $P_{Rx}^{CP,XP}$, for each polarisation (CP or XP) was calculated from the MPCs [18]:

$$P_{Rx}^{CP,XP}\left(t_{[s]}, d_{[m]}, r\right)_{[dBm]} =$$
$$10\log\left(\sum_{i=1}^{N_{MPC}} P_{MPC_i}^{CP,XP}\left(t_{[s]}, d_{[m]}, r\right)_{[W]}\right) + 30 \quad (1)$$

where:

- $N_{MPC}$: number of MPCs of each measurement;
- $P_{MPC_i}^{CP,XP}$: power of the $i^{th}$ MPC component;
- $t$: CIR measurement time;
- $d$: distance to the AP;
- $r$: route.

Since a series of CIR measurements were recorded at different times for each point, the average received power, i.e., the time average at each point, should be taken:

$$\overline{P_{Rx\_t}^{CP,XP}\left(d_{[m]}, r\right)}_{[dBm]} = \overline{P_{Rx}^{CP,XP}\left(t_{i[s]}, d_{[m]}, r\right)}_{[dBm]}\bigg|_t \quad (2)$$

where $N_t$ is the number of time measurements at each point.

### B. Cross-polarisation analysis

The cross-polarisation discrimination ratio, $X_{PD}$, is defined as the ratio between the power received in the CP and the XP channels [17]:

$$X_{PD}\left(t_{[s]}, d_{[m]}, r\right)_{[dB]} =$$
$$P_{Rx}^{CP}\left(t_{[s]}, d_{[m]}, r\right)_{[dBm]} - P_{Rx}^{XP}\left(t_{[s]}, d_{[m]}, r\right)_{[dBm]} \quad (3)$$

where $P_{Rx}^{CP}$ and $P_{Rx}^{XP}$ are the received power in the CP and XP channel respectively.

For each measurement point, the average depolarisation is

$$\overline{X_{PD\_t}\left(d_{[m]}, r\right)}_{[dB]} = \overline{X_{PD\_CIR}\left(t_{[s]}, d_{[m]}, r\right)}_{[dB]}\bigg|_t \quad (4)$$

For Standing, the variation of $\overline{X_{PD\_t}}$ with distance along a route is mainly due to changes in user location, while for Walking it is also due to changes in measurement conditions coming from user mobility, in which case the movement of on-body antennas must be considered. In any case, the average along distance of $\overline{X_{PD\_t}}$ in a given route, $\overline{X_{PD\_td}}$, is an indicator of depolarisation in the route:

$$\overline{X_{PD\_td}\left(r\right)}_{[dB]} = \overline{X_{PD\_t}\left(d_{[m]}, r\right)}_{[dB]}\bigg|_d \quad (5)$$

In addition, the variability of depolarisation along a route is given by the average of $\sigma_{XPD\_td}$ over distance:

$$\overline{\sigma_{XPD\_td}}\left(r\right)_{[dB]} = \sqrt{\frac{1}{N_d}\sum_{i=1}^{N_d}\left(\sigma_{XPD\_t}\left(d_{i[m]},r\right)_{[dB]}\right)^2} \qquad (6)$$

where $N_d$ is the number of measurement points in each route.

It is also of interest to evaluate the aggregated $\overline{X_{PD\_t}}$ for a given case in space, $\overline{X_{PD\_tA}}$, i.e., the $\overline{X_{PD\_t}}$ for a particular on-body antenna placement, polarisation, etc., to account for depolarisation characteristics in a given case:

$$\overline{X_{PD\_tA[dB]}} = \frac{1}{N_A}\sum_{i=1}^{N_A}\overline{X_{PD\_t}}\left(i\right)_{[dB]} \qquad (7)$$

$$\overline{\sigma_{XPD\_tA[dB]}} = \sqrt{\frac{1}{N_A}\sum_{i=1}^{N_A}\left(\sigma_{XPD\_t}\left(i\right)_{[dB]}\right)^2} \qquad (8)$$

The transfer of energy between CP and XP channels is of particular interest when it comes to depolarisation, because it offers the possibility of using orthogonal polarisations in a given channel by using the correlation between these two channels for this purpose. First, the dependence of the received power for the channels CP and XP on the distance is eliminated by fitting a linear regression model. Then the correlation coefficient for a given route, $\rho_{CP,XP}$, between the two polarisations is calculated [19]:

$$\rho_{CP,XP}\left(r\right) = \rho\left(P_{Rx-var}^{CP}\left(d_{[m]},r\right), P_{Rx-var}^{XP}\left(d_{[m]},r\right)\right) \qquad (9)$$

where $P_{Rx-var}^{CP,XP}$ is the variability of the average received power over its linear behaviour,

$$P_{Rx-var}^{CP,XP}\left(d_{[m]},r\right)_{[dBm]} = $$
$$\overline{P_{Rx\_t}^{CP,XP}\left(d_{[m]},r\right)}_{[dBm]} - P_{Rx-lin}^{CP,XP}\left(d_{[m]},r\right)_{[dBm]} \qquad (10)$$

where $P_{Rx-lin}^{CP,XP}$ is the linear regression of $\overline{P_{Rx\_t}^{CP,XP}}$.

## V. DEPOLARISATION ANALYSIS

The analysis of signals depolarisation at the Rx antennas is important for the receiver design. The depolarisation analysis is based on the average of $X_{PD}$ for each route, $\overline{X_{PD\_td}}$, with higher values indicating lower depolarisation. The correlation between the Rx power in the CP and XP channels, $\rho_{CP,XP}$, is a measure of the energy transfer between the two channels along the route (e.g., due to limb movement).

Fig. 2 shows $\overline{X_{PD\_t}}$ for Walking, Approach, route C. Limb movement (AL_L and LL_L) is clearly visible in the variations along the route, while To_F and He_L show more stable curves. Depolarisation is higher for Tx V-Pol, Fig. 2 (a), than for Tx H-Pol, Fig. 2 (b).

Fig. 3 shows the classification of link mobility and the standard deviation of $X_{PD}$ values aggregated by user dynamics, Tx polarisation and on-body antenna. The aggregated standard deviation of $X_{PD}$, $\overline{\sigma_{XPD\_tA}}$, is in the range of [0.48, 0.94] dB for Standing and of [1.39, 2.68] dB for Walking, while for Walking

it is 1.94 and 1.70 dB for Low dynamic links (To_F and He_L) and 2.42 and 2.47 dB for Medium ones (AL_L and LL_L). These values show a clear dependence of $\overline{\sigma_{XPD\_tA}}$ on user mobility (Standing or Walking) and link dynamics (Low or Medium), with a higher $\overline{\sigma_{XPD\_tA}}$ being associated with higher user mobility and link dynamics. Fig. 3 also shows that for H-Pol the values are higher than for V-Pol for all on-body antennas, which is confirmed for both Standing and Walking. Overall, $\overline{\sigma_{XPD\_tA}}$ has a value of 1.83 dB and 2.44 dB for V-Pol and H-Pol, respectively.
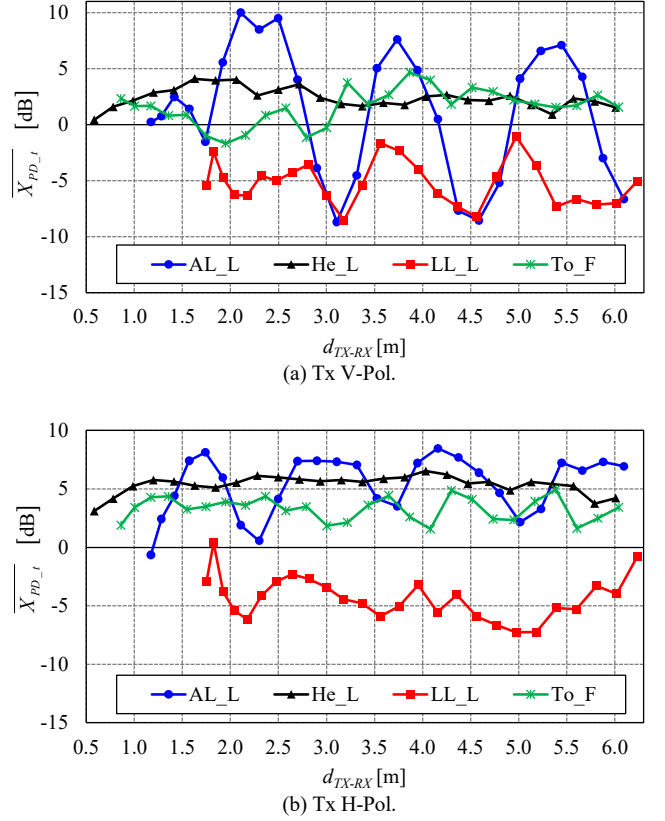


(a) Tx V-Pol.



(b) Tx H-Pol.

Fig. 2. $\overline{X_{PD\_t}}$ for Walking, Approach, Route C.
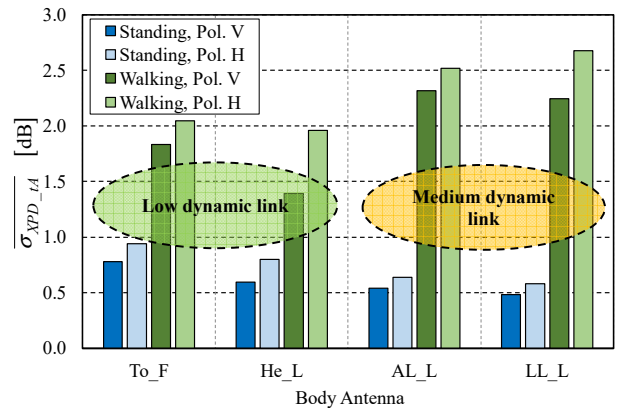


Fig. 3. $\overline{\sigma_{XPD\_tA}}$ and link dynamics.

The average correlation coefficient, $\overline{\rho_{CP,XP}}$ , for Walking is shown in Fig. 4. With the exception of the antenna attached to the arm (AL_L), $\overline{\rho_{CP,XP}}$ has positive values in the range [0.13, 0.73], with He_L having the lowest values in Departure, H-Pol, and LL_L having the highest value in Departure, V-Pol. The negative value of -0.37 for AL_L in Approach, V-Pol indicates a significant energy transfer between the channels due to the pendular movement of the arm. This location is also the one with the largest value deviation in $\overline{\rho_{CP,XP}}$ , i.e., between -0.37 and 0.40.
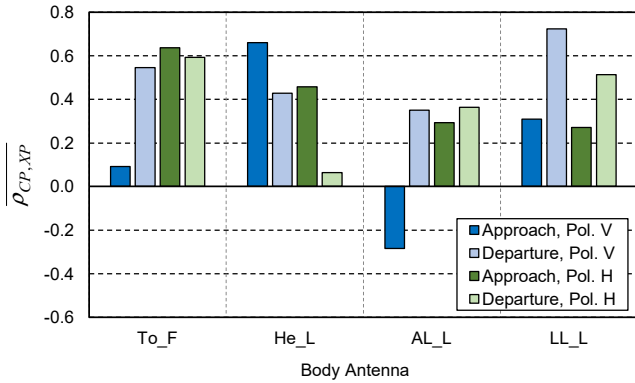


Fig. 4. $\overline{\rho_{CP,XP}}$ for Walking scenarios.

Table IV shows the range of variation Δ (difference between the maximum and the minimum) together with other parameters for Walking. For To_F, He_L and LL_L, $\overline{\rho_{CP,XP}}$ is in the range [0.49, 0.52] and thus almost constant, while for AL_L it is 0.18, which is due to the pendular movement of the arm. The difference between the two orthogonal polarisations in $\overline{\rho_{CP,XP}}$ is quite small (0.42 for V-Pol and 0.44 for H-Pol), as is the case for the routes (0.45 for route C and 0.42 for routes D and W). It can be concluded that there is no significant dependence on polarisation and route. Since 0.5 is normally accepted as a threshold for using diversity [20], it can be concluded that polarisation diversity can be used in this type of environment.

TABLE IV. CP AND XP AVERAGE CORRELATION FOR WALKING.

|  | Range | Δ | $\overline{\rho_{CP,XP}}$ |
|---|---|---|---|
| **To_F** | [0.14, 0.65] | 0.51 | 0.50 |
| **He_L** | [0.13, 0.69] | 0.56 | 0.52 |
| **AL_L** | [-0.37, 0,40] | 0.77 | 0.18 |
| **LL_L** | [0.28, 0.73] | 0.45 | 0.49 |

## VI. DEPOLARISATION MODEL

The dependence of depolarisation on user mobility, polarisation, link dynamics and visibility between antennas was assessed by multivariable linear regression based on the least squares method using Matlab® [19] and [21]. The statistics of the model resulting from this regression show no significant dependence between $\overline{X_{PD\_td}}$ and any of the parameters being considered.

A statistical model for $\overline{X_{PD\_td}}$ , a measure of depolarisation along a route, was obtained by fitting probability density functions to measurement data. Several statistical distributions were tested and the Normal Distribution, with a mean of 2.0 dB and a standard deviation of 4.3 dB, is the best fit. The fit passed the $\chi^2$, the Anderson-Darling and the Kolmogorov-Smirnov tests with a significance value of 0.05 and showed a correlation value of 0.98, [22] and [23].

The dependence of $\overline{\sigma_{XPD\_td}}$ , a measure of average mobility along a route, on user dynamics, Tx polarisation, link mobility and antenna visibility, is represented by a multivariable linear regression that aims to provide an accurate estimate while keeping complexity low, given by:

$$\overline{\sigma_{XPD\_td[dB]}} = 0.66 + \frac{u_m}{u_{m\max}}\left(0.95 + 0.37\,p_{Tx} + 0.62\,\frac{l_d}{l_{d\max}}\right) \quad (11)$$

where:

- $p_{Tx}$ : Tx polarisation (0 if vertical, 1 if horizontal);
- $u_m$ : user mobility (0 m/s for Standing and 1.3 m/s for Walking);
- $l_d$ : link dynamics (0 m/s for Low and 2 m/s for Medium).

This model has a coefficient of determination, $R^2$, of 0.90, an adjusted $R^2$ of 0.89 and a mean square error of 0.27 dB. The residuals are not biased and show a Normal Distribution with a zero mean and a standard deviation of 0.26 dB, passing the $\chi^2$ and the Anderson-Darling tests [24].

The proposed model can be analysed in more detail by looking at the Standing/Walking and V-/H-Pol scenarios. As $\overline{\sigma_{XPD\_td}}$ is a measure of average mobility along the route, the analysis of the model parameters in Table V shows a clear dependence of $\overline{\sigma_{XPD\_td}}$ on user dynamics and an independence of visibility between antennas; it is approximated by a constant value of 0.66 dB in Standing, where the user is at fixed positions, while the value is higher in Walking, but depends on Tx polarisation and link dynamics and is higher for H-Pol.

TABLE V. VALUES OF $\overline{\sigma_{XPD\_td}}$ .

| $u_m$ | $l_d$ | $p_{Tx}$ | $\overline{\sigma_{XPD\_td}}$ [dB] |
|---|---|---|---|
| Standing | --- | --- | 0.66 |
| Walking | Low | V | 1.61 |
|  |  | H | 1.98 |
|  | Medium | V | 2.23 |
|  |  | H | 2.60 |

## VII. CONCLUSIONS

This paper presents an analysis of depolarisation in propagation of BAN communications in an off-body configuration, in an indoor scenario from an Ultra-Wideband measurement campaign using Channel Impulse Responses in the 5.8 GHz band, performed in an empty room at Gdańsk

University of Technology. A fixed Tx antenna was used with vertical and horizontal polarisations, while a user wore dual-polarised Rx antennas on the body, standing at fixed positions or walking towards or away from the Tx antenna along three parallel routes. The cross-depolarisation discrimination ratio, $X_{PD}$, were calculated from the measurements.

The analysis focuses on antenna visibility (classified according to their alignment and body shadowing conditions), link dynamics (classified according to the movement pattern of the on-body antenna) and user mobility (classified according to human mobility, i.e., Standing or Walking). Three visibility conditions were considered: LoS, when both HPBWs of the off-body and on-body antennas are aligned; sOLoS, when the HPBW of the off-body antenna is directed to the back of the on-body antenna and body shadowing is present; and sQLoS, when the off-body and on-body antennas are aligned but their HPBWs are not.

The analysis of depolarisation was based on the average value and on the correlation between the received orthogonal polarisations for each route. The average correlation values for the three routes are almost all positive, with only one exception, for the on-body antenna on the wrist, indicating a significant energy transfer between the channels due to the pendular motion of the arm. The average correlation is in the range [0.35, 0.40], which shows no dependence on polarisation or route and indicates that polarisation diversity can be used as it is below 0.5.

The average $X_{PD}$ for each route is well modelled by a Normal Distribution with a mean of 2.0 dB and a standard deviation of 4.3 dB. In addition, a model is presented for the average standard deviation of $X_{PD}$ as a function of transmitted polarisation, user mobility and link dynamics.

Future work will address the influence of the presence of other people in the environment and their different behaviour, i.e., standing, gesturing, and walking, will be investigated.

## REFERENCES

[1] A. Reichman, J. Takada, D. Bajić, K.Y. Yazdandoost, W. Joseph, L. Martens, C. Roblin, R. D'Errico, C. Oliveira, L.M. Correia and M. Hämäläinen, "Body Communications," in R. Verdone and A. Zanella (eds.), *Pervasive Mobile and Ambient Wireless Communications*, Springer, London, UK, 2012, pp. 609–660.

[2] H.B. Lim, D. Baumann, J. Cai, R. Koh, E.P. Li and Y. Lu, "Antennae Polarization for Effective Transmission of UWB Signal around Human Body," in *Proc. of ICUWB 2007 - IEEE International Conference on Ultra-Wideband*, Singapore, Sep. 2007, DOI: 10.1109/ICUWB.2007.4380945.

[3] M. Berg and T. Tuovinen, "Propagation along a human body surface in WBAN; remarks of desirable antenna characteristics," in *Proc. of MOBIHEALTH 2014 - 4th International Conference on Wireless Mobile Communication and Healthcare*, Athens, Greece, Nov. 2014, DOI: 10.1109/MOBIHEALTH.2014.7015976.

[4] T. Uusitupa and T. Aoyagi, "Analysis of Dynamic On-Body Communication Channels for Various Movements and Polarization Schemes at 2.45 GHz," *IEEE Transactions on Antennas and Propagation*, Vol. 61, No. 12, Dec. 2013, pp. 6168–6179, DOI: 10.1109/TAP.2013.2281369.

[5] T. Tuovinen, M. Berg and E. Salonen, "The effect of antenna pattern and polarization for launching creeping waves on a skin surface," in *Proc. of EuCAP 2014 - 8th European Conference on Antennas and Propagation*, The Hague, Netherlands, Apr. 2014, DOI: 10.1109/EuCAP.2014.6902129.

[6] K.Y. Yazdandoost and R. Miura, "Antenna polarization mismatch in BAN communications," in *Proc. of IMWS-BIO 2013 - IEEE MTT-S International Microwave Workshop Series on RF and Wireless Technologies for Biomedical and Healthcare Applications*, Singapore, Dec. 2013, DOI: 10.1109/IMWS-BIO.2013.6756209.

[7] K. Turbic, S.J. Ambroziak, L.M. Correia and M. Beko, "Wideband Off-Body Channel Characteristics with Dynamic User," in *Proc. of EuCAP 2019 - 13th European Conference on Antennas and Propagation*, Krakow, Poland, Apr. 2019.

[8] S.J. Ambroziak, K. Turbic and L.M. Correia, "Wideband Channel Measurements for Polarised Indoor Off-Body Communications," in *Proc. of URSI-GASS 2021 - XXXIV General Assembly and Scientific Symposium of the International Union of Radio Science*, Rome, Italy, Aug. 2021, DOI: 10.23919/URSIGASS51995.2021.9560191.

[9] P. Tiago and A. Moreira, *UWB antenna design for diversity scenarios*, Technical Report, Instituto Superior Técnico, University of Lisbon, Lisbon, Portugal, Apr. 2015 (https://fenix.tecnico.ulisboa.pt/downloadFile/281870113702347/ExtendedAbstract.pdf).

[10] ITU-R, *Characteristics of ultra-wideband technology*, Recommendation ITU-R SM.1755-0, May 2006 (https://www.itu.int/dms_pubrec/itu-r/rec/sm/R-REC-SM.1755-0-200605-I!!PDF-E.pdf).

[11] Dassault Systems, *CST Studio Suite 3D EM simulation and analysis software*, https://www.3ds.com/products-services/simulia/products/cst-studio-suite, Oct. 2022.

[12] M.M. Ferreira, F.D. Cardoso, S.J. Ambroziak and L.M. Correia, "Influence of User Mobility and Antenna Placement on System Loss in B2B Networks," *IEEE Access*, Vol. 10, Mar. 2022, pp. 37039–37049, DOI: 10.1109/ACCESS.2022.3163859.

[13] Ł. Januszkiewicz, "Analysis of Human Body Shadowing Effect on Wireless Sensor Networks Operating in the 2.4 GHz Band," *Sensors*, Vol. 18, No. 10, Oct. 2018, pp. 3412, DOI: 10.3390/s18103412.

[14] K. Turbic, L.M. Correia and M. Beko, "A Mobility Model for Wearable Antennas on Dynamic Users," *IEEE Access*, Vol. 6, Oct. 2018, pp. 63635–63648, DOI: 10.1109/ACCESS.2018.2877500.

[15] J.J. Fuchs, "Multipath time-delay detection and estimation," *IEEE Transactions on Signal Processing*, Vol. 47, No. 1, Jan. 1999, pp. 237-243, DOI: 10.1109/78.738263.

[16] K. Turbic, *Channel Modelling for Polarised Off-Body Communications with Dynamic Users*, Ph.D. Thesis, Instituto Superior Técnico, University of Lisbon, Lisbon, Portugal, May 2019 (https://grow.tecnico.ulisboa.pt/wp-content/uploads/2019/06/kturbic_thesis.pdf).

[17] ITU-R, *Definitions of terms relating to propagation in non-ionized media*, Recommendation ITU-R P.310-10, Aug. 2019 (https://www.itu.int/dms_pubrec/itu-r/rec/p/R-REC-P.310-10-201908-I!!PDF-E.pdf).

[18] ITU-R, *Multipath propagation and parameterization of its characteristics*, Recommendation ITU-R P.1407-8, Sep. 2021 (https://www.itu.int/dms_pubrec/itu-r/rec/p/R-REC-P.1407-8-202109-I!!PDF-E.pdf).

[19] H. Cramér, *Mathematical methods of statistics*, Princeton University Press, Princeton, NJ, USA, 1999.

[20] Y. Huang and K. Boyle, *Antennas: from theory to practice*, Wiley, Chichester, UK, 2008.

[21] MathWorks, *MathWorks - Makers of MATLAB and Simulink*, https://www.mathworks.com, Jun. 2022.

[22] T.T. Soong, *Fundamentals of probability and statistics for engineers*, John Wiley & Sons, Hoboken, NJ, USA, 2004.

[23] A.M. Mathai and P.N. Rathie, *Probability and statistics*, Macmillan, London, UK, 1977.

[24] J. Frost, *Regression analysis: an intuitive guide for using and interpreting linear models*, Statistics by Jim Publishing, State College, PA, USA, 2020.